Future trends of dissolved inorganic nitrogen concentrations in Northwestern Mediterranean coastal waters under climate change

Regina Temino-Boes [a,*], Rafael García-Bartual[a], Inmaculada Romero[a] and Rabindranarth Romero-Lopez [b]

[a] Instituto de Ingeniería del Agua y del Medio Ambiente, Universitat Politècnica de València, Camino de Vera s/n, Valencia 46022, Spain

[b] Departamento de Ingeniería Civil, Universidad Veracruzana, Lomas del Estadio s/n, Xalapa 91000, Mexico

* Corresponding author: reteboe@doctor.upv.es

Abstract

Coastal ecosystems are amongst the most vulnerable to climate change, due to their location at the land-sea interface. In coastal waters, the nitrogen cycle can be significantly altered by rising temperatures and other factors derived from climate change, affecting phytoplankton and higher trophic levels. This research analyzes the effect of meteorological variables on dissolved inorganic nitrogen (DIN) species in coastal inshore waters of a Northwestern Mediterranean region under climate change. We built simple mathematical schemes based on artificial neural networks (ANN), trained with field data. Then, we used regional climatic projections for the Spanish Mediterranean coast to provide inputs to the trained ANNs, and thus, allowing the estimation of future DIN trends throughout the 21st century. The results obtained indicate that nitrite and nitrate concentrations are expected to decrease mainly due to rising temperatures and decreasing continental inputs. Major changes are projected for the winter season, driven by a rise in minimum temperatures which decrease the nitrite and nitrate peaks observed at low temperatures. Ammonium concentrations are not expected to undergo a significant annual trend but may either increase or decrease during some months. These results entail a preliminary simplified approach to estimate the impact of meteorological changes on DIN concentrations in coastal waters under climate change.

Keywords: Artificial neural networks; Climate change; Coastal waters; Dissolved inorganic nitrogen; Mediterranean Sea.

1. Introduction

Climate change is expected to exacerbate the imbalance of the nitrogen cycle (Gruber and Galloway, 2008), which could already be even greater than expected (Paulmier and Ruiz-Pino, 2009). Coastal areas are known to be particularly vulnerable. In fact, some authors envisage that the future management of nutrient export might have a dramatic impact on coastal water quality (Sinha et al., 2019). Other researchers underline that anthropogenic pressures such as population increase and agricultural practices, plus the cumulative effect of climate change, will probably aggravate nutrient cycling alteration in coastal waters (Rabalais et al., 2009; Sinha et al., 2019). Several investigations outline that nutrient processes will be modified as a response to changes in temperature (Wagena and Easton, 2018), wind patterns (Deng et al., 2018), hydrology, sea level rise (Statham, 2012) and precipitation (Störmer, 2011). Global warming can also contribute to hypoxia in coastal areas by reducing the vertical exchange, making the system more sensitive to nutrient loads (Du et al., 2018). As a consequence of the changes induced, a shift in the relationship between nutrients and phytoplankton should be expected, which might require a re-evaluation of nutrient criteria for ecological status assessment (Liu et al., 2018). Complex interactions among environmental and climate drivers regulate phytoplankton in coastal zones (Pesce et al., 2018), which entails a significant impact of climate change on primary production. The combined effect of higher temperatures and changes in nutrient availability can have drastic consequences for phytoplankton production in coastal waters (Lee et al., 2019), which will add up to the impact of increasing anthropogenic nutrient loadings (Huo et al., 2019). Additionally, the macrobenthos community may also be affected by sea level rise, leading to an increase in nitrogen flux to the water column (Brito et al., 2012).

Dissolved inorganic nitrogen (DIN), i.e. ammonium, nitrite and nitrate, are the most reactive forms of nitrogen in marine waters and play an important role in primary production (Camargo and Alonso, 2006). Nitrate is the most stable form of inorganic nitrogen in oxygenated environments and is generally the dominating form of DIN in estuaries and the surrounding coastal waters (Statham, 2012). Ammonium is also a relevant N species which is often associated to urban influence (Flo et al., 2011). Finally, even though nitrite is the less abundant of the three forms of DIN due to its instability, it is often used as an indicator of the balance between oxidative and reductive reactions (Temino-Boes et al., 2019). As a consequence of climate change, the variations in rainfall patterns may lead to the reduction of DIN inputs to coastal waters through river discharges (Pesce et al., 2018), while processes such as ammonification, nitrification and denitrification could be altered by rising temperatures or ocean acidification (Temino-Boes et al., 2019; Wannicke et al., 2018).

The Mediterranean coast has been identified as one of the most responsive regions to climate change, driven by a significant decrease in the expected mean precipitation (Herrmann et al., 2014). According to some authors, a reduction in the system's biomass can be expected in the Mediterranean Sea during the 21st century (Lazzari et al., 2014), as well as seagrass degradation (Ontoria et al., 2019), surface water warming, salinity increase (Vargas-Yáñez et al., 2017) and a decrease in nutrient availability (Herrmann et al., 2014). On the other hand, renewable water resources are also expected to decrease (García-Ruiz et al., 2011), due to higher rates of sea surface evaporation and reduced rainfall (Romanou et al., 2010), while water demand continues to rise (García-Ruiz et al., 2011; Wang and Polcher, 2019). Under future climate scenarios in the Northwestern Mediterranean Sea, changes in deep water convection mechanisms in winter will likely diminish the importance of nutrient upwelling, whilst horizontal currents will become a more relevant fertilization mechanism (Macias et al., 2018). These alterations may lead to significant changes in both nutrient distribution and phytoplankton community structures (Severin et al., 2014), which in turn could possibly shift towards small-size groups (Herrmann et al., 2014).

Flo et al. (2011) defined coastal inshore waters (CIW) of the Mediterranean Sea as the coastal waters laying between the shore and 200 m into the sea. This reduced region is a unique habitat for many species, and a major socio-economic interest, with tourism activities increasingly threatening the ecosystems (Colella et al., 2016). The Mediterranean CIW are particularly vulnerable to anthropogenic influences, and its characteristics differ considerably from other coastal regions located further into the sea (>200m). Significantly higher DIN concentrations were reported in CIW, where continental influence is the major driver of nitrogen concentrations (Flo et al., 2011), mainly derived from river discharges. The Ebro river delta, the most important delta in the Iberian peninsula, has a mean surface elevation of 0.87 m over the average sea water level, which makes it very sensitive to potential sea level rise, critically threatening nutrient removal dynamics (Genua-Olmedo et al., 2016). Both climate change and agricultural practices have significant impacts on nitrate concentrations in the Ebro basin, while phosphate concentrations are mainly driven by agricultural and industrial practices (Aguilera et al., 2015). In the case of the Jucar River Basin District (Southeast of Spain), temperatures are expected to increase up to 4.86°C in summer by 2040 (Chirivella et al., 2016) and consequently alter nitrogen transformation processes (Temino-Boes et al., 2019).

The aforementioned impacts and the systems implicated are extremely difficult to model successfully due to their inherent complexity and the great number of variables involved. In this context, artificial neural networks (ANN) provide a very attractive modelling framework, which has become increasingly popular, particularly in the evaluation of climate change impacts (Altunkaynak, 2007; Liu et al., 2010). The human brain inspired the mechanisms used for ANNs development. They have been extensively used in many fields, including water quality evaluation (He et al., 2011). One of the main advantages of ANN models in comparison to deterministic models is that an extensive knowledge of the physicochemical processes is not required (He et al., 2011). Besides, ANN models can deal with nonlinear relationships among variables (Liu et al., 2010), improving the accuracy of long-term forecasts (Doğan et al., 2016). The effect of climate change on water resources has been estimated with ANNs in urban areas (Al-Zahrani and Abo-Monasar, 2015), aquifers (Coppola Jr. et al., 2005), deltas (Byakatonda et al., 2016), rivers (Piotrowski et al., 2015), lakes (Altunkaynak, 2007; Doğan et al., 2016) and marine environments (Coutinho et al., 2019). Results show that ANN models often outperform conventional methods (Al-Zahrani and Abo-Monasar, 2015). Nutrient mechanisms, biogeochemical cycling (Bittig et al., 2018) and primary production (Mattei et al., 2018) in the ocean under climate change scenarios have also been evaluated with ANNs .

Nonetheless, only few studies have focused on the forecasting of global warming effects on nutrient cycling in coastal regions (Basu et al., 2010; Wang and Polcher, 2019). In this research, we developed simple ANN modelling schemes as a first approach to evaluate regional climate change impacts on DIN concentrations trends in CIW through meteorological variables. More specifically, we propose a non-linear three-layered feedforward artificial neural network structure, containing a single output node. We trained and tested three different ANN models with such topology with field data, to estimate ammonium, nitrite and nitrate concentrations. Using these trained ANNs expected changes in DIN species concentrations are then estimated, considering two meteorological projections under regional climate change scenarios corresponding to the representative concentrations pathways (RCP) 4.5 and 8.5 (Moss et al., 2010). Due to the necessary simplifications of the physical processes, the results obtained are of qualitative interest rather than quantitative. Our study site is an inshore Mediterranean coastal area of the South East of Spain, exposed to very limited anthropogenic pressures.

2. Materials and Methods

2.1. Study area

The Jucar River Basin District is located in the Spanish Mediterranean coast. In this study we focus in the water body C002 (Figure 1) which is the pristine reference site for the moderately influenced by continental inputs region. The Ebro river delta is located approximately 60 km North from the study site and represents the highest continental water input with a mean annual flow of 286 $m^3.s^{-1}$ for the period 2000-2018. Additionally, the aquifer of El Maestrazgo which has a mean approximate flow of 1.5 $m^3.s^{-1}$, discharges through three submarine springs: Peñíscola, Badum and Alcossebre. Alcossebre is located within our study site, while Badum and

Peñíscola are located 1.5 km and 6 km North from DP134 monitoring site respectively (Garcia-Solsona et al., 2010). As very limited anthropogenic alteration of water quality exists in this area (Romero et al., 2013), it becomes easier to study the effect of physical and meteorological variables on nitrogen concentrations. Five monitoring sites were located within C002, which are presented in Figure 1.

In this study, we focus on coastal inshore waters (0 - 200m from the coast), in which continental influence is the main driver of nutrient concentrations (Flo et al., 2011). The samples collected for the development of this work were taken at <200m from the shore, where the depth is <2m, as described by Flo et al. (2011). As a consequence, the water column is completely mixed, and no stratification exists. Additionally, samples were taken at the surface, which implies that the effect of the sediment can be neglected. The small tidal range in the Mediterranean Sea prevent the dispersion of nutrients into the sea (Flo et al., 2011). Water samples were collected from each monitoring site once per month from February 2006 to January 2011. Samples were taken in plastic bottles at the surface and from beyond the wave breakpoint, refrigerated and carried to the laboratory. The temperature and pH were measured in situ with a YSI 6600 Multi Parameter V2 Sonde. Salinity was measured at the laboratory with a Portasal 8410A salinometer. The samples were filtered with Millipore HAWP filters and DIN concentrations (ammonium, nitrite and nitrate) were analyzed with an Alliance Instruments Integral Futura air-segmented continuous-flow autoanalyzer. Ammonium was measured based on Berthelot's reaction and nitrite with Shinn (1941) water analysis method adapted for seawater by Bendschneider and Robinson (1952). Nitrate was reduced to nitrite with a Cu/Cd reducing column in basic conditions (pH = 8.5), as described by (Grasshoff, 1976). More details are provided by Temino-Boes et al. (2019a). Air temperature, wind speed and rainfall data were obtained from the Ministry of Agriculture, Fisheries and Food, and Ebro river discharges were obtained from the Ebro Water Authority.

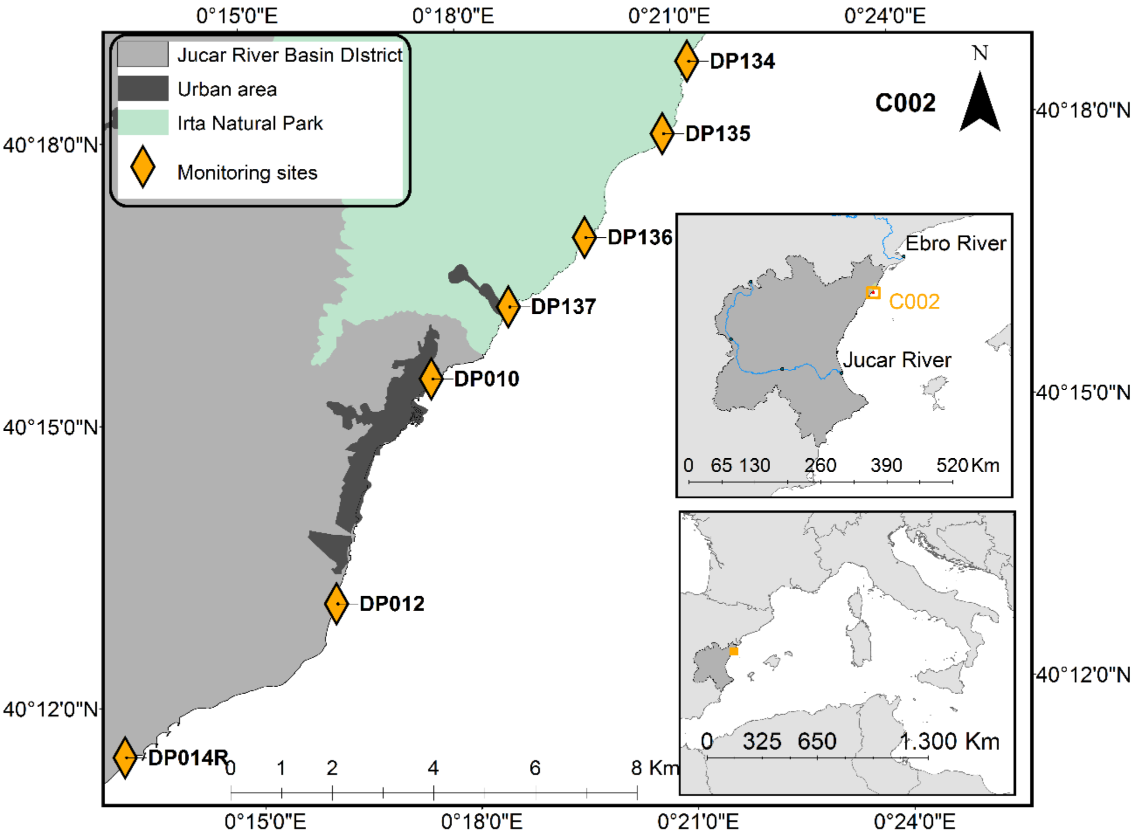

Figure 1. Study site corresponding to the water body C002 identified as reference site of the Jucar River Basin District. The five monitoring sites are shown.

2.2. Data pre-analysis

Considering that continental influence is the main driver of nutrient concentrations (Flo et al., 2011) in CIW of the Northwestern Mediterranean, several physical and meteorological variables were selected as potential input variables to model nutrient concentrations. These variables were: wind speed, rainfall, salinity, Ebro river flow, pH and water temperature. The output sensitivity to input variables relationships can be estimated based on the Spearman rank correlation if a nonlinear but monotonic relationship is assumed (Pianosi et al., 2016). In order to determine to which variables nitrogen concentrations are more sensitive, we calculated the Spearman rank correlation coefficients. The results of this analysis were used to select the most appropriate input variables to the model.

Rainfall can significantly affect nitrogen in CIW through different processes: by diluting nutrient concentrations, through river runoff or through submarine groundwater discharge (SGD). Nitrogen discharges through SGD have been reported to be significant in the study area (Garcia-Solsona et al., 2010), particularly in the form of nitrate (Ballesteros et al., 2007). The aquifer of El Maestrazgo, which discharges through coastal springs in Irta National Park, is mainly recharged through rainfall infiltration (Ballesteros et al., 2007). The time lag between SGD flux response to freshwater infiltrated has been reported to be ∼3 months (Garcia-Solsona et al., 2010). In order to determine the time lag between rainfall and nitrate concentrations in our model, we calculated the cross-correlation with R version 3.5.1.

2.3. Artificial neural networks

ANN are data-driven models that have shown to be very successful modelling tools in a diversity of research areas (Abrahart et al., 2004; Alanis et al., 2019; Govindaraju, 2000; Lek and Guégan, 1999). In particular, they have proved to be very efficient in the prediction of relevant variables in complex systems characterized by nonlinear dependencies of data, as it is the case of the ones analyzed herein. Several ANN schemes were trained in this research, in order to extract the most relevant interactions between the measured variables and synthesize them through simple network topologies. These ANN schemes are built with the final aim of simulating long-term future expectable trends in the system under different climatic scenarios, as other authors have proposed (Abdullahi and Elkiran, 2017; Elgaali and Garcia, 2007). These modelling steps can also be helpful to gain a better understanding of the studied system behavior and its internal relationships between the involved physical variables mentioned before. The type of ANNs employed herein is the well-known feed forward multilayer perceptron of three layers with supervised learning, trained with the classical error-backpropagation learning algorithm (Gardner and Dorling, 1998; Rumelhart et al., 1986).

The structure of the networks is made up of three layers: an input layer comprising a group of explanatory variables, a hidden layer with nodes including non-linear activation functions, and an output layer corresponding to a selected target variable to be predicted. The training process of the networks allows to configure the network internal weights in order to minimize the error function, in this case, the average squared error with respect to the measure (known values) of the target variable. The activation function used for the hidden nodes was the popular logistic function (Kohonen, 1988):

$$\varphi(x) = \frac{1}{1+e^{-x}} \tag{1}$$

Where x is the input value to the particular node, resulting from operations in previous layers and connections to the node. $\varphi(x)$ is the value produced by the activation function, i.e., output of the particular node under consideration.

The choice of the number of hidden nodes (n_h) affects the training process and the effectiveness and final performance of the network. Complex relationships between inputs and outputs are difficult to be captured with too few hidden nodes, while too many hidden nodes may result in network over-training and a loss of generalization capacity of the network. Due to the sample size available for this study, the option for a parsimonious model is generally recommended. According to it, we applied the criteria (Lachtermacher and Fuller, 1994), adopting the minimum n_h value matching this criteria:

$$\frac{1.1 \cdot N}{10} \leq n_h \cdot (I + 1) < \frac{3 \cdot N}{10} \tag{2}$$

where *N* is the sample size, and *I* is the number of input variables.

The data used for network training is the sample corresponding to the period from February 2006 to January 2010, while the period from February 2010 to January 2011 is reserved for validation. This partition is consistent with the criteria suggested by Haykin (1999):

$$r_{VAL} = 1 - \frac{\sqrt{2 \cdot W - 1} - 1}{2 \cdot (W - 1)} \tag{3}$$

where *W* is the number of weights in the neural network, and r_{VAL} is the proportion of the total data used for training.

As it is the case with other black-box models, the overall performance is highly influenced by the data preprocessing (Nawi et al., 2013). In particular, the computational efficiency of the networks is enhanced if both input and output variables are scaled. Consequently, all variables involved in the ANN modelling were previously pre-process through equation (4).

$$x' = \left(\frac{x - x_{MIN}}{x_{MAX} - x_{MIN}} \right)^{\gamma} \tag{4}$$

where *x* represents the original variable, x_{MIN} is the minimum value, x_{MAX} is the maximum value of the sample, *x'* is the transformed variable, and γ is an exponent introduced in order to reduce the final skewness. γ values are conveniently chosen for each of the variables considered in the ANN modelling process, ranging from 0.3 to 1.0.

The back-propagation algorithm was used to train all the networks. This sequential iterative method adjusts the network weights in small steps, following the direction of negative gradient of the error function. The learning rate was manually modified to smaller values as the training process advanced, to avoid undesirable oscillatory behavior of the training error function. During the learning process, the order of presentation of patterns was randomized through the shuffling of the cases, which is usually advantageous to avoid local minima. While other more powerful and quicker algorithms are commonly used (Burney et al., 2007), the reduced size of the networks involved herein allowed an efficient use of the simpler error-backpropagation algorithm until the error function reached a specified convergence with satisfactory quickness. Training and validation processes of the different ANNs proposed were performed using the software STATISTICA.

2.4. Climate change scenarios

The National Plan for Adaptation to Climate Change (PNACC), through the Scenarios-PNACC initiative, collects regional climate information for Spain, both of current climate and of future scenarios for the next decades. The projections of meteorological variables are based on the Fifth Assessment Report (AR5) of the Intergovernmental Panel on Climate Change (IPCC). The initiative integrates the results of international dynamic and statistic regionalization projects such as Euro-CORDEX and VALUE, with national projections developed by the National Meteorological Agency (AEMET) and by the Meteorology Group of Santander (CSIC - University of Cantabria). We downloaded projections of daily meteorological variables for future emission scenarios from the Platform of Exchange and Consultation of Information on Adaptation to Climate Change in Spain (AdapteCCA.es), under RCP4.5 and RCP8.5. Mean monthly estimations for air temperature, humidity and rainfall were calculated from 2011 to 2100 for both RCPs.

Due to the lack of water temperature and salinity projections under climate change in the study area a simplified approach to estimate these variables is necessary. Linear stepwise regression models were used to estimate salinity and water temperature from meteorological variables, i.e. air temperature, rainfall and humidity. For the estimation of salinity also Ebro river flow was used. All variables were previously normalized through a unity-based normalization. The first 4 years of measurements were used for model calibration and the last year for validation. The Spanish center for studies and experimentation of public works (CEDEX) assessed the impact of climate change on water resources in a natural regime in the Spanish basins throughout the 21st century. The model developed is the Integrated Precipitation Simulation model (SIMPA), a distributed simulation model of the hydrological cycle that establishes water balances for the different processes. It estimates the contribution from meteorological data and the physical characteristics of the territory. The model is fed with regionalized projections of climate change procured by AEMET and provides the expected values of the main hydrological variables. The results are available online through a downloadable computer application (CAMREC), a plugin for QGIS 2.18. The changes expected in the Ebro river flow at its mouth throughout the 21st century under RCP 4.5 and RCP 8.5 were obtained from CAMREC.

Monthly DIN concentrations from 2011 to 2100 were estimated by means of the developed ANN model. For each month, Mann-Kendall trend test was applied to determine whether the trends observed are statistically significant. This test is a non-parametric monotonic trend analysis which identifies the increasing or decreasing patterns in time series data (Chaudhuri and Dutta, 2014; Colella et al., 2016). The magnitude of the trend was evaluated with Sen's slope (Sen, 1968), a non-parametric method which does not require assumptions on the normal distribution of the data (Kitsiou and Karydis, 2011). The annual trend is evaluated with the season Mann-Kendall test and the seasonal Sen's slope. These tests are performed with the package "trend" in R version 3.5.1.

3. Results

3.1. Monitoring data

The data obtained from the monitoring campaigns are presented in Figure 2. Water temperature and pH are similar between monitoring sites. Salinity however is lower in DP010 which can be attributed to SGD inputs. DIN concentrations are higher in DP010, nitrate concentrations particularly. This monitoring site is located close to an urban area as opposed to the other sites which are within Irta National Park. Additionally, the SGD in this area entails an input of DIN especially in the form of nitrate (Ballesteros et al., 2007). As indicated in section 2.2., the cross-correlation between nitrate and rainfall was evaluated. The result of the analysis is presented in Figure 3. The correlation is maximum with a time-lag of 4 months between rainfall and nitrate concentrations. This finding is in close agreement with the time lag in the aquifer's discharge time in Garcia-Solsona et al. (2010) which also studied the same aquifer of El Maestrazgo, and indicated a time lag of approximately 3 months. The Spearman correlations between physicochemical variables and DIN concentrations is shown in Table 1. Based on these correlations the input variables selected for DIN species estimation were water temperature, salinity and rainfall (with a 4-month time lag). Ebro river flow, the pH and the wind speed were discarded for not having any significant correlation.

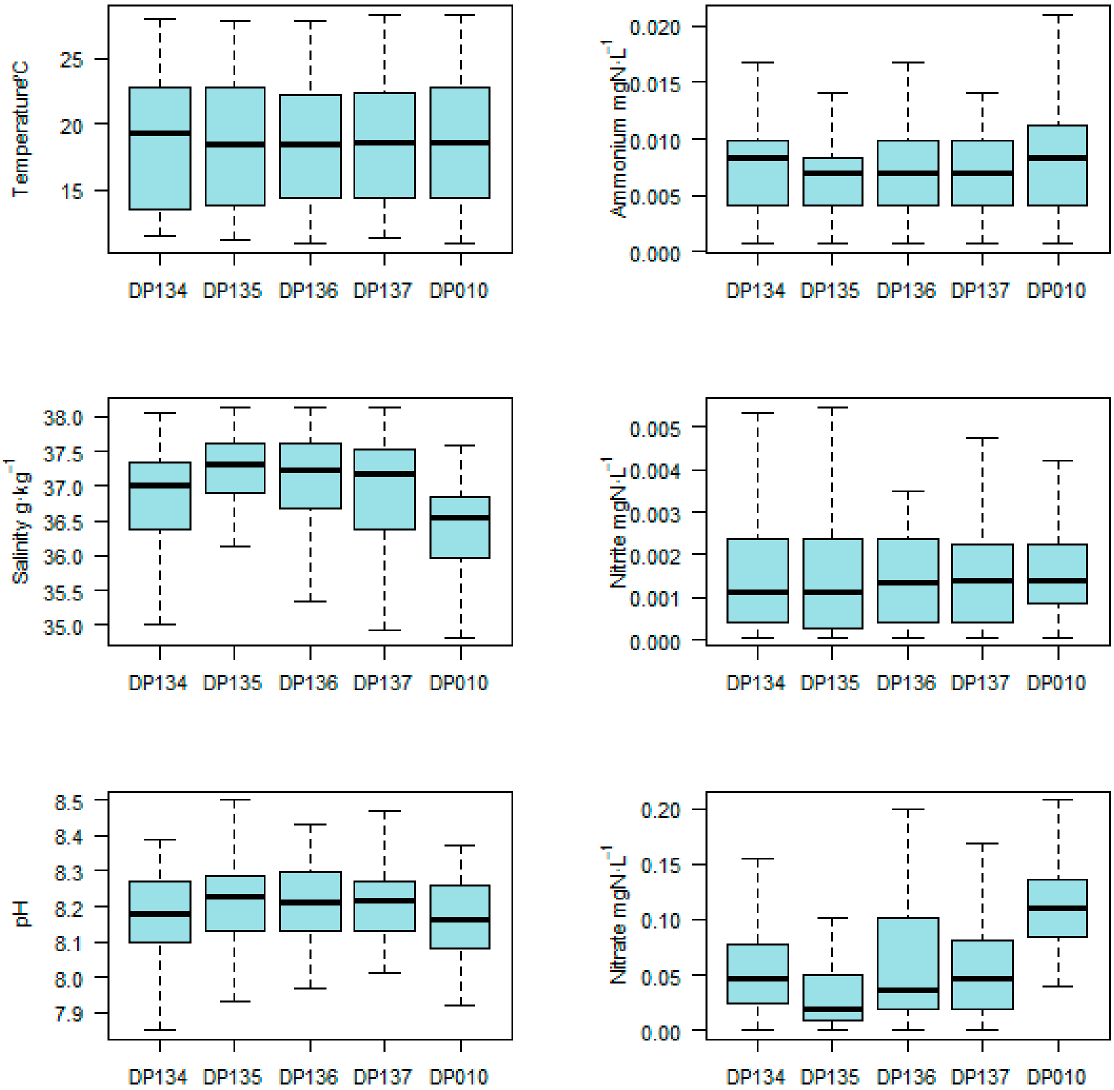

Figure 2. Boxplot of water temperature, salinity and pH (left) and dissolved inorganic nitrogen species concentrations (right) obtained during monthly monitoring campaigns from February 2006 to January 2011. The median is represented by a black horizontal line, the bottom and the top of the box represent the first (Q1) and third quartiles (Q3) respectively and the lower and upper ends of the whisker represent Q1-1.5 (Q3-Q1) and Q3 + 1.5 (Q3-Q1) respectively. Outliers are not represented.

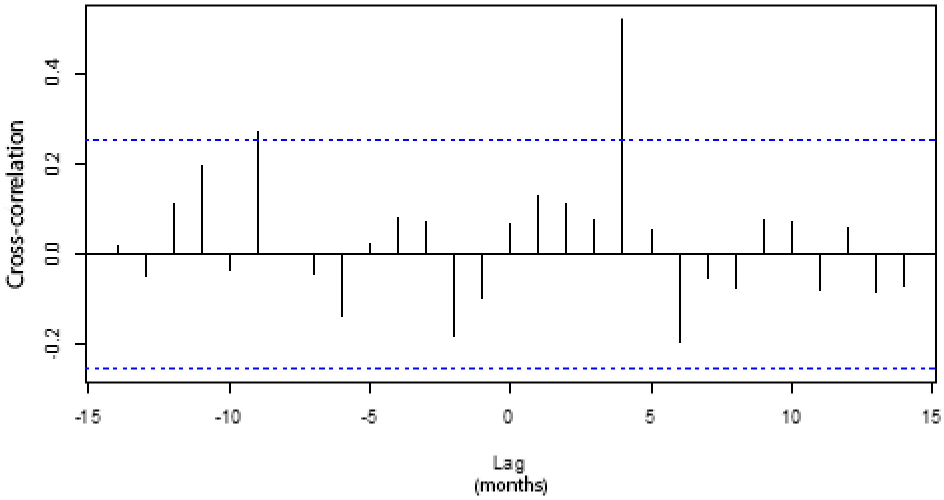

Figure 3. Cross-correlation between nitrate concentration and rainfall. Horizontal axis shows the time lag in nitrate concentrations (months) while vertical axis shows the correlation between nitrate and rainfall for each lag.

Table 1. Spearman rank correlations between studied variables. NH_4^+ is ammonium in mgN·L^{-1}, NO_2^- is nitrite in mgN·L^{-1}, NO_3^- is nitrate in mgN·L^{-1}, R-4 is rainfall in mm.day^{-1}with a 4-month time lag, Q is Ebro river flow in m^3·s^{-1}, WT is water temperature in °C, S is salinity in g·kg^{-1} and W is wind speed in m·s^{-1}. The asterisk indicates a statistically significant correlation at a 0.05 significant level.

	NH_4^+	**NO_2^-**	**NO_3^-**	**R-4**	**Q**	**WT**	**pH**	**S**	**W**
NH_4^+	-	-0.05	0.23	0.19	0.09	0.25*	0.10	-0.39*	-0.07
NO_2^-		-	0.43*	0.19	0.06	-0.54*	-0.05	-0.11	0.03
NO_3^-			-	0.46*	0.23	-0.33*	0.10	-0.64*	-0.16
R-4				-	0.32*	-0.02	0.16	-0.37*	-0.06
Q					-	-0.35*	-0.04	-0.46*	-0.04
WT						-	0.29*	0.12	-0.02
pH							-	-0.08	-0.14
S								-	0.20
W									-

3.2. ANN Model

A simple artificial neural network architecture is proposed to predict values of each of the DIN species, i.e., NH_4^+, NO_3^- and NO_2^-. One network is built and trained for each of these variables, although the three networks developed have the same 3-layer topology. The variables used as predictors, that is, the input variables of the networks, are the same for each of the three neural networks. The selected predictors are those physical parameters that showed higher correlation: salinity, temperature and rainfall. Consequently, the number of nodes in the input layer is three, and the number of nodes in the output layer is one. The number of hidden nodes was calculated with equation (2), resulting in n_h=2, which is also consistent with recommendation by (Wanas et al., 1998). This network size proved to be optimal, as other networks with n_h=1, 3 and 4 were later tested, yielding to worse performance indexes. Consequently, the architecture of the proposed ANN consists on a 3-layer feedforward neural network with 3 input nodes, two hidden nodes and one output node (either NH_4^+, NO_3^- or NO_2^-), as indicated in Figure 4. The obtained rooted mean squared errors (RMSE) for training and validation data are presented in Table 2. While Figure 5 shows the model outputs for ammonium, nitrite and nitrate and the R^2 for each model.

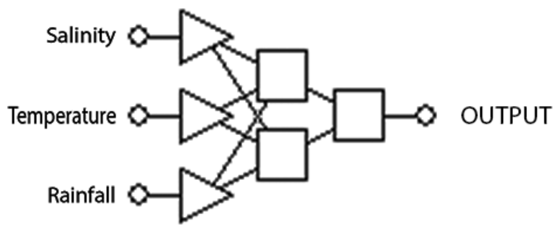

Figure 4. Feedforward neural network topology with the three input variables and the output (either NH_4^+, NO_3^- or NO_2^-)

Table 2. Rooted mean squared error (RMSE) in $mgN{\cdot}L^{-1}$ for training and validation data in the three models with outputs NH_4^+, NO_3^- or NO_2^- respectively.

RMSE	**NH_4^+**	**NO_2^-**	**NO_3^-**
Training	4.10E-03	1.48E-03	2.63E-02
Validation	3.15E-03	8.15E-04	1.99E-02

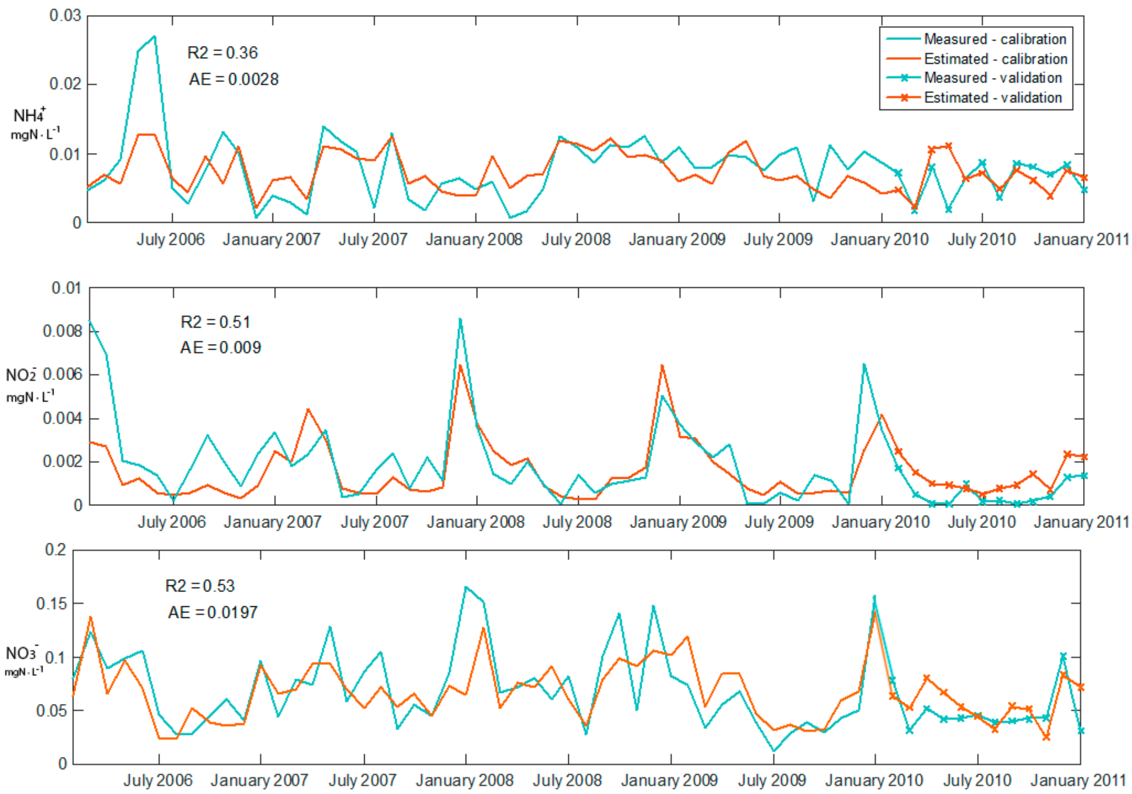

Figure 5. Ammonium (NH_4^+), nitrite (NO_2^-) and nitrate (NO_3^-) models based on artificial neural networks. Rainfall with a 4-month time lag, water temperature and salinity are the input variables. The coefficient of determination R^2 and the absolute error (AE) in $mgN.L^{-1}$ is shown.

3.3. Water temperature and salinity models

Linear regression model parameters to estimate water temperature and salinity are presented in Table 3. Water temperature is estimated from air temperature solely, while salinity is estimated with rainfall (with a 4-month time lag), humidity and Ebro river flow. Both models are found to be statistically significant as determined by the R^2, adjusted-R^2 and p-value shown in Table 4. Durbin-Watson statistic tests the residuals to determine if there is any significant correlation based on the order in which they occur in the data. There is no serial autocorrelation in the residual at a 95% level of significance as indicated in Table 3. As indicated in section 2.4, the first 48 measurements corresponding to the first 4 years were used to build the model and the last 12 values were used for validation. Both calibration and validation data are shown in Figure 6. The coefficient of determination R^2 was very similar in calibration and validation for both models.

Table 3. Results of the stepwise linear regressions to estimate water temperature (model 1) and salinity (model 2). T_{air} is air temperature, R-4 is rainfall with a 4-month time lag, H is humidity and Q is Ebro river flow.

Model	Parameter	Estimate	Standard Error	T statistic	p-value
1: Water Temperature	Constant	0.1032	0.0242	4.2700	0.0001
	Tair	0.8944	0.0424	21.0767	0.0000
2: Salinity	Constant	0.9476	0.0651	14.5534	0.0000
	R-4	-0.1927	0.0947	-2.0353	0.0479
	H	-0.2734	0.0996	-2.7454	0.0087
	Q	-0.5436	0.1055	-5.1549	0.0000

Table 4. Model interpretations of stepwise linear regressions to estimate water temperature (model 1) and salinity (model 2): coefficient of determination, standard error, Durbin-Watson statistics and ANOVA.

Parameter	Model 1: Water temperature	Model 2: Salinity
R^2	90.62	50.99
R^2 adjusted	90.41	47.65
Standard error	0.0937	0.1589
Durbin-Watson statistic	1.9702	1.5951
Durbin-Watson p-value	0.4079	0.0722
ANOVA F-Ratio	444.23	15.26
ANOVA p-value	0.0000	0.0000

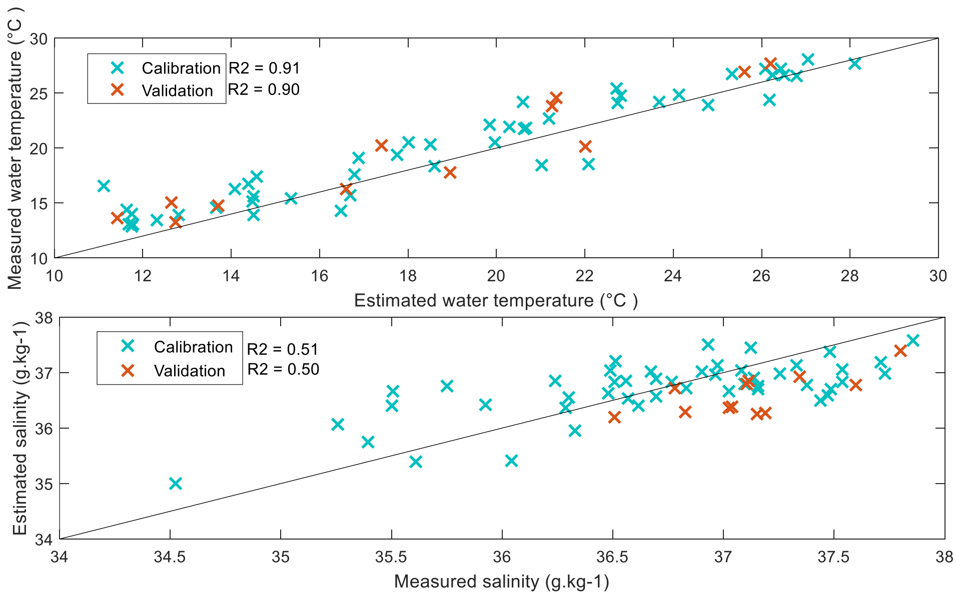

Figure 6. Stepwise linear regression models for the estimation of water temperature (up) and salinity (down). The coefficient of determination R^2 and the absolute error (AE) are shown for both calibration and validation data.

3.4. The effect of climate change on DIN concentrations

Estimations of air temperature, humidity and rainfall from 2011 to 2100 under climate change scenarios were downloaded from AdapteCCA.es website and changes in Ebro river flow were obtained from CAMREC as mentioned in section 2.4. The changes projected for these variables under climate change each month for the period 2070-2100 relative to 1971-2000 (1961-2000 for Ebro river flow) are presented in Figure 7. Salinity and water temperatures for both RCP 4.5 and RCP 8.5 emission scenarios were calculated with the linear models developed in the previous section. By means of the ANN models, DIN concentration trends between 2011 and 2100 were estimated. Results are represented in Figure 8.

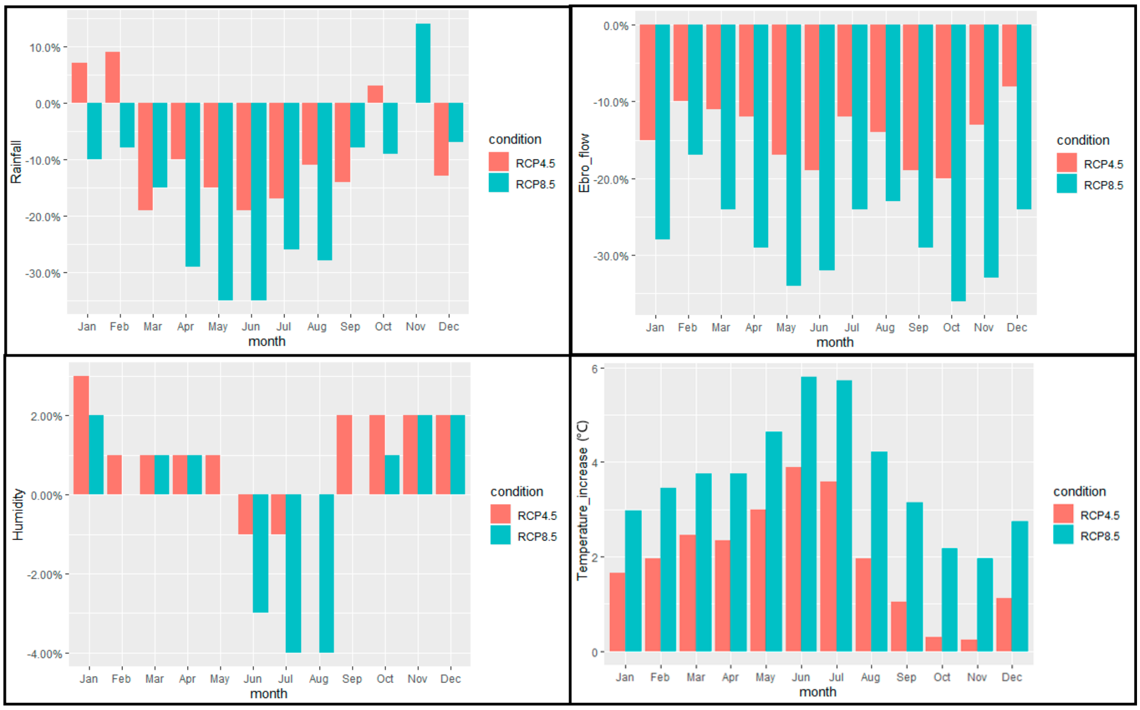

Figure 7. Changes in air temperature, rainfall, humidity and Ebro river flow for the period 2070-2100 compared to 2071-2000 (2061-2000 for Ebro river flow) under RCP 4.5 and RCP 8.5 scenarios.

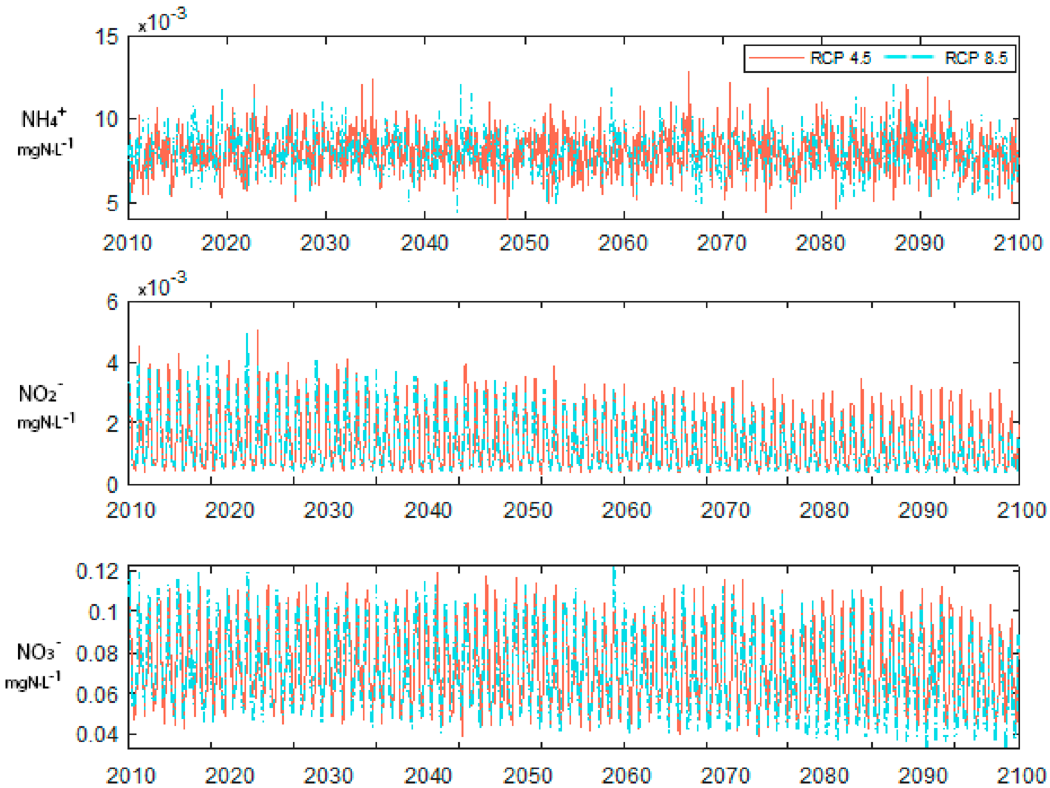

Figure 8. Projections of ammonium, nitrite and nitrate concentrations from 2011 to 2100 by means of the ANN models under RCP 4.5 and RCP 8.5 scenarios.

The Sen's slope for each month was calculated to measure the magnitude of the increasing or decreasing trend for DIN species over the period 2011 to 2100. Additionally, Mann-Kendall test was applied to evaluate whether the observed trend is statistically significant. The results are shown in Table 5. Nitrite and nitrate concentrations are expected to decrease both under RCP 4.5 and RCP 8.5 on an annual basis, with greater decrease found for RCP 8.5. Nitrite peaks, which are observed under low temperature conditions, are expected to decline. On the other hand, ammonium is expected to increase mainly between January and March and decrease from September to December, but the global trend was not statistically significant.

Table 5. Sen's slope for monthly changes in nitrate, nitrite or ammonium concentrations between 2011 and 2100 projections for each month under RCP 4.5 and RCP 8.5. The annual trend is evaluated with the seasonal Sen's slope.

Month	NH_4^+ 4.5	NO_2^- 4.5	NO_3^- 4.5	NH_4^+ 8.5	NO_2^- 8.5	NO_3^- 8.5
January	7.14E-06**	-1.18E-05**	-4.65E-05*	7.89E-06**	-2.16E-05**	-1.94E-04**
February	2.94E-06	-5.06E-06**	-4.06E-05	2.00E-05**	-1.33E-05**	-1.91E-04**
March	7.32E-06*	-3.44E-06**	-1.53E-05	9.09E-06**	-5.88E-06**	-1.66E-04**
April	-4.76E-06	-3.13E-06**	-6.40E-05*	-2.99E-06	-4.76E-06**	-1.19E-04**
May	4.35E-06	0.00E+00	-4.17E-05	4.35E-06	-3.33E-06**	-1.32E-04**
June	0.00E+00	-1.20E-07**	-6.64E-05**	-2.99E-06	-1.47E-06**	-1.56E-04**
July	2.56E-06	-9.04E-07**	-5.37E-05**	2.18E-06	-1.80E-06**	-1.75E-04**
August	4.76E-08	-8.88E-07**	-6.86E-05**	1.19E-05**	-2.48E-06**	-1.83E-04**
September	2.41E-06	-1.46E-06**	-5.29E-05**	-1.46E-06**	-3.23E-06**	-1.90E-04**
October	-8.54E-06*	-2.21E-06**	-7.43E-05**	-8.96E-06**	-4.64E-06**	-1.85E-04**
November	-9.87E-06*	-4.13E-06**	-8.59E-06**	-1.80E-05**	-8.59E-06**	-1.66E-04**
December	-7.28E-06	-1.08E-05**	-9.36E-05**	-1.21E-05**	-2.43E-05**	-1.84E-04**
Annual	2.34E-07	-2.34E-06**	-5.84E-05**	2.35E-06	-5.22E-06**	-1.64E-04**

*Statistically significant correlation at a 0.05 significance level
** Statistically significant correlation at a 0.01 significance level

4. Discussion

Artificial neural networks have proved to be a useful tool to evaluate the effects of climate change on DIN species. The proposed models showed the ability to estimate the impact of future meteorological conditions on the trends of DIN concentrations in CIW. Nonetheless, the results should be interpreted cautiously due to the assumptions made throughout the evaluation. Nitrite and nitrate models reached R^2 values over 0.50, which can be acceptable, considering the high variability generally found in coastal waters. Due to the high uncertainty in ammonium concentrations in Northwestern Mediterranean coastal waters (Paches et al., 2019), the model performance was lower for this nutrient (Figure 5). Also, the additional uncertainty introduced by the linear models developed for water temperature and salinity estimations should be pointed out. Water temperature model reached R^2 = 0.90; but salinity model had R^2 = 0.50, implying a degree of uncertainty introduced to ANN model inputs for future projections. The observed errors in ANN outputs can be attributed to both natural and anthropogenic sources. Anthropogenic nitrogen inputs, even if considered to be very limited in our study area (Romero et al., 2013), may account for some of the uncertainties. For instance, nitrogen inputs through Ebro river or submarine groundwater discharges are not constant along the year. On the other hand, the discharges of the aquifer El Maestrazgo are related to other parameters on top of precipitation. Nonetheless, the main contribution of this work lies in the evaluation of the overall expected tendency of nitrogen concentrations under climate change scenarios.

In this sense, and according to the modelling results obtained, nitrite and nitrate concentrations are expected to drop under both RCP 4.5 and RCP 8.5 climate change scenarios, with greater decreases under RCP 8.5. Nitrite peaks generally occur due to low temperatures which decouple both steps of nitrification (Temino-Boes et al., 2019). In accordance with this, future projections show a reduction of peaks during December and January, mainly due to the expected increase in minimum temperatures. We also observed a high negative correlation between temperature and nitrite concentrations (-0.54). Overall, the decaying trend of nitrite levels under climate change scenarios is basically driven by future rising temperatures, while the decrease in continental inputs (salinity and rainfall) play a secondary role. Nitrate is also expected to decrease, driven by both higher temperatures and decreasing rainfall. It is interesting to note that maximum monthly cumulative rainfall occurs in September, resulting in higher aquifer recharge during this month. This yields to groundwater discharge peaks during successive months, with an average time delay of 4 months, i.e., January. A decrease of future expected rainfall, more particularly during this rainiest month, will result in significant groundwater discharges reduction, which in turn will affect nitrate levels. This is consistent with simulation results obtained under RCP 8.5, where the most significant decreases in future nitrate concentration are expected during January.

The expected trends derived from the presented simulations herein, are consistent with known processes governing the dynamics of the nitrogen cycle. As pointed out by previous researchers, higher nitrification and denitrification rates are actually driven by higher temperatures, and thus, are expected to decrease future nitrogen availability (Wagena and Easton, 2018). Other authors already indicated that changes in temperature and precipitation could decrease nitrogen yields in coastal waters (Alam et al., 2017). Some studies point out a significant imbalance of the ocean's nitrogen budget, with greater losses than inputs (Voss et al., 2013). Bi et al. (2018) also found a negative correlation between nitrogen concentrations and temperature. Precipitation was also correlated to nitrogen concentration in previous studies, indicating that climate change might reduce nitrogen loads (Bi et al., 2018). Concerning ammonium concentrations, our results indicate that significant changes are not expected on an annual basis. While ammonification and other related processes are intensified due to higher temperatures, other factors are counteracting such effect, such as lower future precipitation and lower river discharges. Not being simultaneous drivers, though, smaller changes and trend fluctuations are expected for individual months.

The modelling framework presented herein necessary implies an important over-simplification of the complex systems under investigation. It neglects certain underlying physicochemical processes involved, and therefore, many uncertainty sources need to be accounted for. Although most relevant climatic drivers were considered in the analysis, other pressures such as changes in anthropogenic nutrient loads were not taken into consideration. For instance, 65% of the Ebro delta is occupied by rice fields (Genua-Olmedo et al., 2016), which implies that nutrient management in agriculture is a key factor for future export of DIN (Jennerjahn, 2012). The future fertilization policy applied in the Ebro catchment is uncertain, ranging from a 10% increase to a 15% decrease (Herrero et al., 2018). Obviously, the sort and amount of fertilizer will change due to changes in rainfall and air temperatures, which would influence coastal nutrient loads (Statham, 2012). Socioeconomic decisions about land use and management will have determining consequences for hydrological processes (Zarzuelo et al., 2019) and thus, on coastal nutrient enrichment (Sinha et al., 2019). Clearly, an interdisciplinary collaboration is necessary between natural and social sciences (Jennerjahn, 2012). Another aspect to be outlined is the highly regulated Ebro river, affecting its average discharges to the Mediterranean. About 96% of the catchment is regulated by dams (Jiménez et al., 2017), causing significant reductions of river flow over the past decades (Fatorić and Chelleri, 2012). In the future, higher water regulation due to increasing water demand (Wang and Polcher, 2019) and more intense human activity is generally expected in the Mediterranean region (Herrero et al., 2018). Depletion of river flows in the delta areas may enhance saline intrusion in the lower reaches of rivers and into the groundwater reserves (García-Ruiz et al., 2011). Under such conditions, the vulnerability of the Ebro valley will likely increase (Barrera-Escoda et al., 2014), influencing the nitrogen export to coastal waters. Natural and human-induced hydrodynamic alterations (Zarzuelo et al., 2019) may also have a significant impact on nutrient discharges. Furthermore, the potential changes in phytoplankton community and their ability to assimilate nitrogen induced by higher temperatures was not considered in this study (Kumar et al., 2018).

In spite of these limitations, the study area selected corresponds to an area of low anthropogenic inputs (Romero et al., 2013) which indicates that climate change may have a greater impact than changes derived from direct human inputs.

On a global scale, the alteration of nitrogen transformations leads to many complex cascading effects (Gruber and Galloway, 2008). Overall, the results obtained in this study indicate that climate change is expected to decrease DIN concentrations in Mediterranean CIW due to increasing temperatures and lower continental inputs. The results obtained are of practical interest for management purposes, but the limitations of a simplified analysis should be recognized. Future studies should focus on the development of more sophisticated models with a combined evaluation of climate change and changes in anthropogenic nutrient loads.

5. Conclusion

The modelling approach proposed herein, together with the results derived from the performed simulations, represent a first approach to evaluate the potential climate change impact on dissolved inorganic nitrogen concentrations in coastal inshore waters (<200m). More specifically, we focused on the effect of the main meteorological variables on DIN species in the CIW of a Northwestern Mediterranean region with low anthropogenic inputs. As such, quantitative conclusions are necessarily limited, as many uncertainty sources need to be accounted for, as explained previously.

In order to evaluate the impact of climate change on DIN concentrations, we used artificial neural network models trained with real field data collected monthly during a period of 5 years. The most relevant climatic variables were considered as drivers. Results indicate that nitrite and nitrate concentrations are expected to decrease under climate change scenarios RCP 4.5 and RCP 8.5. Cold months such as December, January and February are expected to undergo the major concentration changes due to rising temperature and decreasing continental inputs. Ammonium did not show a significant annual tendency but may increase from January to March and decrease from September to December. Future research should focus on the evaluation of the combined effects of climate change and other human induced changes such as river flow regulations or nitrogen pollution. The evaluation of future nitrogen dynamics in coastal waters with more complex approaches is essential in order to develop preventive action plans.

Acknowledgments: We acknowledge the Valencian Ministry of the Environment, Water, Urban Planning and Housing for their support in field data collection. We also acknowledge the National Meteorological Agency (AEMET) and by the Meteorology Group of Santander (CSIC -

University of Cantabria) for their National Plan for Adaptation to Climate Change (PNACC), from whom meteorological variables for future climate change scenarios were obtained. We thank the Ministry of Agriculture, Fisheries and Food for historical values of air temperature and rainfall, and the Ebro Water Authority for historical Ebro river discharges. Finally, we acknowledge Universitat Politècnica de València for the student scholarship which supported this research.

Funding: Field data collection was supported by the Valencian Ministry of the Environment, Water, Urban Planning and Housing. The work was partly supported by a Cotutelle PhD scholarship granted by Universitat Politècnica de València.

References

Abdullahi, J., Elkiran, G., 2017. Prediction of the future impact of climate change on reference evapotranspiration in Cyprus using artificial neural network. Procedia Comput. Sci. 120, 276–283. doi:10.1016/j.procs.2017.11.239

Abrahart, R.J., Kneale, P.E., See, L.M., 2004. Neural networks for hydrological modelling. Balkema.

Aguilera, R., Marcé, R., Sabater, S., 2015. Detection and attribution of global change effects on river nutrient dynamics in a large Mediterranean basin. Biogeosciences 12, 4085–4098. doi:10.5194/bg-12-4085-2015

Al-Zahrani, M.A., Abo-Monasar, A., 2015. Urban residential water demand prediction based on artificial neural networks and time series models. Water Resour. Manag. 29, 3651–3662. doi:10.1007/s11269-015-1021-z

Alam, M.J., Goodall, J.L., Bowes, B.D., Girvetz, E.H., 2017. The Impact of Projected Climate Change Scenarios on Nitrogen Yield at a Regional Scale for the Contiguous United States. JAWRA J. Am. Water Resour. Assoc. 53, 854–870. doi:10.1111/1752-1688.12537

Alanis, A., Arana-Daniel, N., Lopez-Franco, C., 2019. Artificial neural networks for engineering applications. Academic Press.

Altunkaynak, A., 2007. Forecasting surface water level fluctuations of lake van by artificial neural networks. Water Resour. Manag. 21, 399–408. doi:10.1007/s11269-006-9022-6

Ballesteros, B., Marina, M., Mejías, M., Domínguez, J., 2007. Caracterización hidroquímica del acuífero carbonatado profundo de El Maestrazgo (Castellón).[Hydrochemical characterisation of the deep, carbonated El Maestrazgo aquifer (Castellón)]. Coast. aquifers challenges Solut. 549–564.

Baron, J.S., Hall, E.K., Nolan, B.T., Finlay, J.C., Bernhardt, E.S., Harrison, J.A., Chan, F., Boyer, E.W., 2013. The interactive effects of excess reactive nitrogen and climate change on aquatic ecosystems and water resources of the United States. Biogeochemistry 114, 71–92. doi:10.1007/s10533-012-9788-y

Barrera-Escoda, A., Gonçalves, M., Guerreiro, D., Cunillera, J., Baldasano, J.M., 2014. Projections of temperature and precipitation extremes in the North Western Mediterranean Basin by dynamical downscaling of climate scenarios at high resolution (1971–2050). Clim. Change 122, 567–582. doi:10.1007/s10584-013-1027-6

Basu, N.B., Destouni, G., Jawitz, J.W., Thompson, S.E., Loukinova, N. V., Darracq, A., Zanardo, S., Yaeger, M., Sivapalan, M., Rinaldo, A., Rao, P.S.C., 2010. Nutrient loads exported from managed catchments reveal emergent biogeochemical stationarity. Geophys. Res. Lett. 37, n/a-n/a. doi:10.1029/2010GL045168

Bendschneider, K., Robinson, R.J., 1952. A new spectrophotometric determination of nitrite in sea water. J. Mar. Res. 2, 87–96.

Bi, W., Weng, B., Yuan, Z., Ye, M., Zhang, C., Zhao, Y., Yan, D., Xu, T., 2018. Evolution Characteristics of Surface Water Quality Due to Climate Change and LUCC under Scenario Simulations: A Case Study in the Luanhe River Basin. Int. J. Environ. Res. Public Health 15. doi:10.3390/ijerph15081724

Bittig, H.C., Steinhoff, T., Claustre, H., Fiedler, B., Williams, N.L., Sauzède, R., Körtzinger, A., Gattuso, J.-P., 2018. An Alternative to Static Climatologies: Robust Estimation of Open Ocean CO2 Variables and Nutrient Concentrations From T, S, and O2 Data Using Bayesian Neural Networks. Front. Mar. Sci. 5, 328. doi:10.3389/fmars.2018.00328

Brito, A.C., Newton, A., Tett, P., Fernandes, T.F., 2012. How will shallow coastal lagoons respond to climate change? A modelling investigation. Estuar. Coast. Shelf Sci. 112, 98–104. doi:10.1016/J.ECSS.2011.09.002

Burney, S.M.A., Jilani, T.A., Ardil, C., 2007. A comparison of first and second order training algorithms for artificial neural networks. Int. J. Comput. Inf. Eng. 1, 145–151.

Byakatonda, J., Parida, B.P., Kenabatho, P.K., Moalafhi, D.B., 2016. Modeling dryness severity using artificial neural network at the Okavango Delta, Botswana. Glob. Nest J. 18, 463–481.

Camargo, J.A., Alonso, Á., 2006. Ecological and toxicological effects of inorganic nitrogen pollution in aquatic ecosystems: A global assessment. Environ. Int. 32, 831–849. doi:10.1016/J.ENVINT.2006.05.002

Chaudhuri, S., Dutta, D., 2014. Mann-Kendall trend of pollutants, temperature and humidity over an urban station of India with forecast verification using different ARIMA models. Environ. Monit. Assess. 186, 4719–4742. doi:10.1007/s10661-014-3733-6

Chirivella, V., Capilla, J.E., Pérez-Martín, M.A., 2016. Dynamical versus statistical downscaling for the generation of regional climate change scenarios at a Western Mediterranean basin: The Júcar River District. J. Water Clim. Chang. 7, 379–392. doi:10.2166/wcc.2015.207

Colella, S., Falcini, F., Rinaldi, E., Sammartino, M., Santoleri, R., 2016. Mediterranean ocean colour chlorophyll trends. PLoS One 11, 1–17. doi:10.1371/journal.pone.0155756

Coppola Jr., E.A., Rana, A.J., Poulton, M.M., Szidarovszky, F., Uhl, V.W., 2005. A neural network model for predicting aquifer water level elevations. Ground Water 43, 231–241.

Coutinho, F.H., Thompson, C.C., Cabral, A.S., Paranhos, R., Dutilh, B.E., Thompson, F.L., 2019. Modelling the influence of environmental parameters over marine planktonic microbial communities using artificial neural networks. Sci. Total Environ. 677, 205–214. doi:10.1016/j.scitotenv.2019.04.009

Deng, J., Paerl, H.W., Qin, B., Zhang, Y., Zhu, G., Jeppesen, E., Cai, Y., Xu, H., 2018. Climatically-modulated decline in wind speed may strongly affect eutrophication in shallow lakes. Sci. Total Environ. 645, 1361–1370. doi:10.1016/J.SCITOTENV.2018.07.208

Doğan, E., Kocamaz, U.E., Utkucu, M., Yıldırım, E., 2016. Modelling daily water level fluctuations of Lake Van (Eastern Turkey) using Artificial Neural Networks. Fundam. Appl. Limnol. / Arch. für Hydrobiol. 187, 177–189. doi:10.1127/fal/2015/0736

Du, J., Shen, J., Park, K., Wang, Y.P., Yu, X., 2018. Worsened physical condition due to climate change contributes to the increasing hypoxia in Chesapeake Bay. Sci. Total Environ. 630, 707–717. doi:10.1016/J.SCITOTENV.2018.02.265

Elgaali, E., Garcia, L.A., 2007. Using Neural Networks to Model the Impacts of Climate Change on Water Supplies. J. Water Resour. Plan. Manag. 133. doi:10.1061/(ASCE)0733-9496(2007)133:3(230)

Fatorić, S., Chelleri, L., 2012. Vulnerability to the effects of climate change and adaptation: The case of the Spanish Ebro Delta. Ocean Coast. Manag. 60, 1–10. doi:10.1016/J.OCECOAMAN.2011.12.015

Flo, E., Garcés, E., Manzanera, M., Camp, J., 2011. Coastal inshore waters in the NW Mediterranean: Physicochemical and biological characterization and management implications. Estuar. Coast. Shelf Sci. 93, 279–289. doi:10.1016/j.ecss.2011.04.002

García-Ruiz, J.M., López-Moreno, I.I., Vicente-Serrano, S.M., Lasanta-Martínez, T., Beguería, S., 2011. Mediterranean water resources in a global change scenario. Earth-Science Rev. 105, 121–139. doi:10.1016/j.earscirev.2011.01.006

Garcia-Solsona, E., Garcia-Orellana, J., Masqué, P., Rodellas, V., Mejías, M., Ballesteros, B., Domínguez, J.A., 2010. Groundwater and nutrient discharge through karstic coastal springs (Castelló, Spain). Biogeosciences 7, 2625–2638. doi:10.5194/bg-7-2625-2010

Gardner, G.W., Dorling, S.R., 1998. Artificial neural networks (the multilayer perceptron)—a review of applications in the atmospheric sciences. Atmos. Environ. 32, 2627–2636.

Genua-Olmedo, A., Alcaraz, C., Caiola, N., Ibáñez, C., 2016. Sea level rise impacts on rice production: The Ebro Delta as an example. Sci. Total Environ. 571, 1200–1210. doi:10.1016/j.scitotenv.2016.07.136

Govindaraju, R.S., 2000. Artificial neural networks in hydrology. Water Science and Technology Library.

Grasshoff, K., 1976. Methods of seawater analysis. Verlag Chemie: Weinstein, New York.

Gruber, N., Galloway, J.N., 2008. An Earth-system perspective of the global nitrogen cycle. Nature 451, 293–296. doi:10.1038/nature06592

Haykin, S., 1999. Neural networks, a comprehensive foundation. Prentice Hall International, Inc.

He, J., Valeo, C., Chu, A., Neumann, N.F., 2011. Stormwater quantity and quality response to climate change using artificial neural networks. Hydrol. Process. 25, 1298–1312. doi:10.1002/hyp.7904

Herrero, A., Gutiérrez-Cánovas, C., Vigiak, O., Lutz, S., Kumar, R., Gampe, D., Huber-García, V., Ludwig, R., Batalla, R., Sabater, S., 2018. Multiple stressor effects on biological quality elements in the Ebro River: Present diagnosis and predicted responses. Sci. Total Environ. 630, 1608–1618. doi:10.1016/j.scitotenv.2018.02.032

Herrmann, M., Estournel, C., Adloff, F., Diaz, F., 2014. Impact of climate change on the northwestern Mediterranean Sea pelagic planktonic ecosystem and associated carbon cycle. J. Geophys. Res. Ocean. 119, 5815–5836. doi:10.1002/jgrc.20224

Huo, S., Zhang, H., Ma, C., Xi, B., Zhang, J., He, Z., Li, X., Wu, F., 2019. Algae community response to climate change and nutrient loading recorded by sedimentary phytoplankton pigments in the Changtan Reservoir, China. J. Hydrol. 571, 311–321. doi:10.1016/J.JHYDROL.2019.02.005

Jennerjahn, T.C., 2012. Biogeochemical response of tropical coastal systems to present and past environmental change. Earth-Science Rev. 114, 19–41. doi:10.1016/J.EARSCIREV.2012.04.005

Jiménez, J.A., Valdemoro, H.I., Bosom, E., Sánchez-Arcilla, A., Nicholls, R.J., 2017. Impacts of sea-level rise-induced erosion on the Catalan coast. Reg. Environ. Chang. 17, 593–603. doi:10.1007/s10113-016-1052-x

Kitsiou, D., Karydis, M., 2011. Coastal marine eutrophication assessment: A review on data analysis. Environ. Int. 37, 778–801. doi:10.1016/J.ENVINT.2011.02.004

Kohonen, T., 1988. An introduction to neural computing. Neural Networks 1, 3–16.

Kumar, S., Bhavya, P.S., Ramesh, R., Gupta, G.V.M., Chiriboga, F., Singh, A., Karunasagar, I., Rai, A., Rehnstam-Holm, A.S., Edler, L., Godhe, A., 2018. Nitrogen uptake potential under different temperature-salinity conditions: Implications for nitrogen cycling under climate change scenarios. Mar. Environ. Res. 141, 196–204. doi:10.1016/j.marenvres.2018.09.001

Lachtermacher, G., Fuller, J.D., 1994. Backpropagation in hydrological time series forecasting.

In: Hipel, K.W., McLeod, A.I., Panu, U.S., Singh, V.P. (Eds.), Stochastic and Statistical Methods in Hydrology and Environmental Engineering. Kluwer Academic, Dordrecht.

Lazzari, P., Mattia, G., Solidoro, C., Salon, S., Crise, A., Zavatarelli, M., Oddo, P., Vichi, M., 2014. The impacts of climate change and environmental management policies on the trophic regimes in the Mediterranean Sea: Scenario analyses. J. Mar. Syst. 135, 137–149. doi:10.1016/j.jmarsys.2013.06.005

Lee, K.H., Jeong, H.J., Lee, K., Franks, P.J.S., Seong, K.A., Lee, S.Y., Lee, M.J., Hyeon Jang, S., Potvin, E., Suk Lim, A., Yoon, E.Y., Yoo, Y. Du, Kang, N.S., Kim, K.Y., 2019. Effects of warming and eutrophication on coastal phytoplankton production. Harmful Algae 81, 106–118. doi:10.1016/J.HAL.2018.11.017

Lek, S., Guégan, J.F., 1999. Artificial neural networks as a tool in ecological modelling, an introduction. Ecol. Modell. 120, 65–73.

Liu, L., Ma, C., Huo, S., Xi, B., He, Z., Zhang, H., Zhang, J., Xia, X., 2018. Impacts of climate change and land use on the development of nutrient criteria. J. Hydrol. 563, 533–542. doi:10.1016/J.JHYDROL.2018.06.039

Liu, Z.L., Peng, C.H., Xiang, W.H., Tian, D.L., Deng, X.W., Zhao, M.F., 2010. Application of artificial neural networks in global climate change and ecological research: An overview. Chinese Sci. Bull. 55, 3853–3863. doi:10.1007/s11434-010-4183-3

Macias, D., Garcia-Gorriz, E., Stips, A., 2018. Deep winter convection and phytoplankton dynamics in the NW Mediterranean Sea under present climate and future (horizon 2030) scenarios. Sci. Rep. 8, 6626. doi:10.1038/s41598-018-24965-0

Mattei, F., Franceschini, S., Scardi, M., 2018. A depth-resolved artificial neural network model of marine phytoplankton primary production. Ecol. Modell. 382, 51–62.

Moss, R.H., Edmonds, J.A., Hibbard, K.A., Manning, M.R., Rose, S.K., Van Vuuren, D.P., Carter, T.R., Emori, S., Kainuma, M., Kram, T., Meehl, G.A., Mitchell, J.F.B., Nakicenovic, N., Riahi, K., Smith, S.J., Stouffer, R.J., Thomson, A.M., Weyant, J.P., Wilbanks, T.J., 2010. The next generation of scenarios for climate change research and assessment. Nature 463, 747–756. doi:10.1038/nature08823

Nawi, N.M., Atomi, W.H., Rehman, M.Z., 2013. The effect of data pre-processing on optimized training of artificial neural networks. Procedia Technol. 11, 32–39.

Ontoria, Y., Gonzalez-Guedes, E., Sanmartí, N., Bernardeau-Esteller, J., Ruiz, J.M., Romero, J., Pérez, M., 2019. Interactive effects of global warming and eutrophication on a fast-growing Mediterranean seagrass. Mar. Environ. Res. 145, 27–38. doi:10.1016/j.marenvres.2019.02.002

Paches, M., Aguado, D., Martínez-Guijarro, R., Romero, I., 2019. Long-term study of seasonal changes in phytoplankton community structure in the western Mediterranean (Valencian Community). Environ. Sci. Pollut. Res. 26, 14266–14276. doi:10.1007/s11356-019-04660-x

Paerl, H.W., 2018. Why does N-limitation persist in the world's marine waters? Mar. Chem. 206, 1–6. doi:10.1016/J.MARCHEM.2018.09.001

Paulmier, A., Ruiz-Pino, D., 2009. Oxygen minimum zones (OMZs) in the modern ocean. Prog. Oceanogr. 80, 113–128. doi:10.1016/J.POCEAN.2008.08.001

Pesce, M., Critto, A., Torresan, S., Giubilato, E., Santini, M., Zirino, A., Ouyang, W., Marcomini, A., 2018. Modelling climate change impacts on nutrients and primary production in coastal waters. Sci. Total Environ. 628–629, 919–937. doi:10.1016/J.SCITOTENV.2018.02.131

Pianosi, F., Beven, K., Freer, J., Hall, J.W., Rougier, J., Stephenson, D.B., Wagener, T., 2016. Sensitivity analysis of environmental models: A systematic review with practical workflow. Environ. Model. Softw. 79, 214–232. doi:10.1016/J.ENVSOFT.2016.02.008

Piotrowski, A.P., Napiorkowski, M.J., Napiorkowski, J.J., Osuch, M., 2015. Comparing various artificial neural network types for water temperature prediction in rivers. J. Hydrol. 529, 302–315.

Rabalais, N.N., Turner, R.E., Diaz, R.J., Justic, D., 2009. Global change and eutrophication of coastal waters. ICES J. Mar. Sci. 66, 1528–1537. doi:10.1093/icesjms/fsp047

Romanou, A., Tselioudis, G., Zerefos, C.S., Clayson, C.A., Curry, J.A., Andersson, A., 2010. Evaporation-precipitation variability over the mediterranean and the black seas from satellite and reanalysis estimates. J. Clim. 23, 5268–5287. doi:10.1175/2010JCLI3525.1

Romero, I., Pachés, M., Martínez-Guijarro, R., Ferrer, J., 2013. Glophymed: An index to establish the ecological status for the Water Framework Directive based on phytoplankton in coastal waters. Mar. Pollut. Bull. 75, 218–223. doi:10.1016/j.marpolbul.2013.07.028

Rumelhart, D.E., Hinton, G.E., Williams, R., 1986. Learning representations by back-propagating errors. Nature 323, 533–536.

Sen, P.K., 1968. Estimates of the Regression Coefficient Based on Kendall's Tau. J. Am. Stat. Assoc. 63, 1379–1389. doi:10.1080/01621459.1968.10480934

Severin, T., Kessouri, F., Rembauville, M., Sánchez-Pérez, E.D., Oriol, L., Caparros, J., Pujo-Pay, M., Ghiglione, J.-F., D'Ortenzio, F., Taillandier, V., Mayot, N., De Madron, X.D., Ulses, C., Estournel, C., Conan, P., 2014. Open-ocean convection process: A driver of the winter nutrient supply and the spring phytoplankton distribution in the Northwestern Mediterranean Sea. J. Geophys. Res. Ocean. 122, 4587–4601. doi:10.1002/jgrc.20224

Shinn, M.B., 1941. Colorimetric method for the determination of nitrite. Ind. Eng. Chem. Anal. Ed. 13, 33–35.

Sinha, E., Michalak, A.M., Calvin, K. V., Lawrence, P.J., 2019. Societal decisions about climate mitigation will have dramatic impacts on eutrophication in the 21st century. Nat. Commun. 10, 939. doi:10.1038/s41467-019-08884-w

Statham, P.J., 2012. Nutrients in estuaries — An overview and the potential impacts of climate change. Sci. Total Environ. 434, 213–227. doi:10.1016/J.SCITOTENV.2011.09.088

Störmer, O., 2011. Climate Change Impacts on Coastal Waters of the Baltic Sea, in: Global Change and Baltic Coastal Zones. Springer, Dordrecht, pp. 51–69. doi:10.1007/978-94-007-0400-8_4

Temino-Boes, R., Romero, I., Pachés, M., Martinez-Guijarro, R., Romero-Lopez, R., 2019. Anthropogenic impact on nitrification dynamics in coastal waters of the Mediterranean Sea. Mar. Pollut. Bull. 145, 14–22. doi:10.1016/j.marpolbul.2019.05.013

Vargas-Yáñez, M., García-Martínez, M.C., Moya, F., Balbín, R., López-Jurado, J.L., Serra, M., Zunino, P., Pascual, J., Salat, J., 2017. Updating temperature and salinity mean values and trends in the Western Mediterranean: The RADMED project. Prog. Oceanogr. 157, 27–46. doi:10.1016/j.pocean.2017.09.004

Voss, M., Bange, H.W., Dippner, J.W., Middelburg, J.J., Montoya, J.P., Ward, B., 2013. The marine nitrogen cycle: recent discoveries, uncertainties and the potential relevance of climate change. Philos. Trans. R. Soc. Lond. B. Biol. Sci. 368, 20130121. doi:10.1098/rstb.2013.0121

Wagena, M.B., Easton, Z.M., 2018. Agricultural conservation practices can help mitigate the impact of climate change. Sci. Total Environ. 635, 132–143. doi:10.1016/J.SCITOTENV.2018.04.110

Wanas, N., Auda, G., Kamel, M.S., Karray, F., 1998. On the optimal number of hidden nodes in a neural network, in: IEEE Canadian Conference on Electric and Computer Engineering Proceedings. pp. 918–921.

Wang, F., Polcher, J., 2019. Assessing the freshwater flux from the continents to the Mediterranean Sea. Sci. Rep. 9, 8024. doi:10.1038/s41598-019-44293-1

Wannicke, N., Frey, C., Law, C.S., Voss, M., 2018. The response of the marine nitrogen cycle to ocean acidification. Glob. Chang. Biol. 24.

Zarzuelo, C., D’Alpaos, A., Carniello, L., López-Ruiz, A., Díez-Minguito, M., Ortega-Sánchez, M., 2019. Natural and Human-Induced Flow and Sediment Transport within Tidal Creek Networks Influenced by Ocean-Bay Tides. Water 11, 1493.